Journal of Structural Engineering and Geotechnics,
8(2), 31-44, Summer 2018

Liquefaction Hazard assessment using Horizontal-to-Vertical Spectral Ratio of Microtremor

Mehdi Mokhberi[*,a], Sadegh Yazdanpanah Fard[b]

[a] *Department of civil engineering, Estahban Branch, Islamic azad University, Shiraz , Iran*

[b] *Department of civil engineering, Estahban Branch, Islamic azad University, Estahban, Iran*

Received 23 July 2018, Accepted 29 November 2018

Abstract

In this paper, the spectral ratio of mmicrotremor, HSVR, is presented for estimating the liquefaction potential of layered soil in the coastal area of the Persian Gulf, which consists of a hard sandstone layer situated between two saturated sandy layers. The surface layer is thin, with a thickness between 2 and 5 meters. The purpose of this paper is to identify the relation between the liquefaction potential, the natural frequency and the amplification factor values using microtremors. Liquefaction assessment was done at 27 stations using the HVSR approach provided by Nakamura [1]. HVSR analysis was carried out using the Geopsy software. According to the results of the analysis, the predominant frequency values range from about 0.8 Hz to 2.4 Hz and the amplification factor values range from 1.1 to 2.8. Based on these parameters, the vulnerability index Kg is determined, which can be used as a parameter in calculating the liquefaction potential of an area. The results show that the vulnerability index is related to the sedimentary depth as well as the frequency and amplification factor. Furthermore, the calculated results confirm that the southern area of Bushehr City, which is larger than other areas, has a high liquefaction potential. Furthermore, it is possible to determine the limit of Kg to estimate the liquefaction hazard. Comparing the results confirms that in Bushehr, a soil layer is liquefiable if its related Kg value is over 1.7. This value may change with the conditions of the layer and the soil specification.

Keywords: *Soil liquefaction, microtremor HVSR, predominant frequency, amplification factor, vulnerability index.*

1. Introduction

During recent decades, huge earthquakes have occurred around the world and killed or injured a number of people and destroyed many buildings. Experience shows that the disastrous effects of earthquakes remain for several years. Therefore, it is necessary to design safe and accurate programs to ensure a safe habitat.

In order to manage earthquake disasters, it is first necessary to understand the nature of these phenomena. Building damage, landslides, slope slips and soil liquefaction are occurrences that are considered in the assessment of earthquake hazards. One common disaster during an earthquake is liquefaction. During earthquakes which occur in coastal regions, it has been observed that liquefaction disasters are more destructive than the main earthquake damage.

*Corresponding Author Email address: mehdimokhberi@gmail.com

The Michoacan earthquake of 1985 destroyed Mexico City, which was built on a former swamp alluvial plain [2]. Earthquakes in Iran (Manjil and Rudbar, 1991) and Turkey (Kocaeli, 1999) have caused severe structural damage and killed more than 50,000 people in the alluvial plains. In Japan, the effect of the material sediment in the 1995 Kobe earthquake events devastated housing, as well as the general and modern infrastructure of Kobe City and the surrounding areas. Finally, the Bantul earthquake of May 27, 2006 killed more than 4,500 people and damaged more than 100,000 homes in the fluvio volcanic plains of Bantul Graben[3]. As an example, in the Northridge earthquake the liquefaction increased the failures by 30%.

The liquefaction potential has been investigated with several approaches. A simplified procedure has been used to predict the liquefaction potential of soils worldwide. It was originally developed by Seed and Idris using the Standard Penetration Test

(SPT)[4]. Since then, this procedure has undergone several revisions and has been updated[5] [6]. In addition, other procedures have been developed based on the Cone Penetration Test (CPT)[7, 8], Becker Penetration Test (BPT) [9], and small-strain Shear Wave Velocity (Vs) measurements[9]. Among them, the Vs is suitable for determining the liquefaction resistance because both the Vs and liquefaction resistance are influenced by factors such as confining stress, plasticity and relative density and the Vs can be measured by several seismic tests including downhole, cross-hole and spectral ratio analysis of the surface.

2. Research Location and Geological Conditions

Microtremor measurements and geotechnical evaluations were carried out in Bushehr region in the south of Iran, in the north part of the Persian Gulf. This port consists of three separate districts, Bushehr City, the city of Tangak and the city of Bahmani. Bushehr is a large city with a long coast and a harbour. Based on Iran's geological zonation, Bushehr province is located in the Zagros zone. The Bushehr area has a simple structure which is confined to NW-SE trending smooth folds, and which is consistent with the Zagros general trend. Mesozoic and Cenozoic units have outcropped; however, Neogene sediments have mostly covered the area. Information about the Zagros basement originates from gravity-meter and aeromagnetic measurements on the Arabian plate, stratigraphic surveys, and data about the Central Iran Basement, the salt domes, and the Hormoz rock fragments. Considering all the data, it is believed that the Zagros basement is the continuation of the N-NE Arabian-Nubian shield that enters Hejaz from NE Africa and is exposed to the western territories and continues to the east of Saudi Arabia under the sediments and lies below the Zagros Basin with a gentle slope related to the Dezful area. The studies conducted in the area have shown that the upper interface of the Zagros basement is very rough and has a complicated topography. The numerous tensional faults have been affected and reflected as surface and/or near-surface thrusts. The Persian Gulf coast and its islands should be regarded as a part of the folded Zagros. According to the measurements performed, the lower interface of the basement lies between 35 and 55 km deep, and it is known that the basement is 25–50 km thick.

In the studied area, faults can be classified into three categories of reverse faults with a northwest-southeast orientation; along the north-south orientation of the right strike-slip faults, which is one of the most fundamental deformation factors of the region, and relatively modest faults associated with region folds. The existing faults in the region include the Kazeroon fault, Borazjan fault and the mountain forehead fault (MFF). Figure 1 shows the active faults in the studied area.

The oldest recorded earthquake that occurred in the Bushehr province was in 1925. The longitude and latitude of the earthquake epicenter were 28.54 N and 51.82 E, respectively. Its magnitude was 5.3 on the Mb scale. The latest recorded earthquake in Bushehr occurred in April 20, 2013 with a magnitude of 6.3 Mb at a depth of 12 km from the surface in Dashti City. The epicenter of this earthquake was 90 km from Bushehr port. The highest level of destruction was reported in Shanbeh City with 90%. The earthquake killed 37 people, injured 1100 and destroyed 3100 buildings[10].

3. Measurement and Analysis

3.1. Geotechnical data

a. General layering based on geological aspect

In this study, geotechnical data have been selected from 32 boreholes of the geotechnical database of the Road and Urban Organization of Bushehr. These data

contain detailed information on the type of soil, soil specific gravity, groundwater level and fine grain content, shear wave velocity, SPT values, etc. Figure 2 illustrates the location of the selected boreholes in the studied area. On this basis, in general, four layers in the region can be identified:

1. Layer of loose soil: This thin layer has different types of aggregates and thicknesses in different parts of the area. The northern and coastal parts consist of coastal sand, and silty and clayey sedimentary soil. In the northern parts, compacted silty and clay soils dominate. In the higher part, outcrops of the layer beneath are seen.

Figure 1. Map of active faults around the studied area (after IIEES, 2003)

2. Cap rock layer: Quaternary marine terraces are the newest hardened sediments in the region of the northern coasts of the Persian Gulf and Oman Sea, including the studied area. This sedimentary cover is a cap rock layer consisting of weak marl-silty formations and low limestone strength sandstones which are in a horizontal position or are slightly sloping towards the sea. These rocks are composed of coral deposits, lime and sandstones containing large parts of marine shells. They are generally deposited in the tidal region to the seafront and usually form a hardened layer at the surface.
3. Sandstone layer: This layer is about 4 to 8 meters thick and consists of two parts: soft sandstone in the upper part and hard marl sandstone in the lower part, separated from each other by a thin layer of clay.
4. Marl and clayey rocks with interlayers of marl and sandstones: Marlins and clay of this layer have an acceptable resistance to undercurrent and dry conditions, but when they are exposed to water or air they quickly lose their resistance and become weathered. This phenomenon is observed to some extent in the sandstone layers.

b. Earth layering according to geotechnical aspect

Overall, the four layers observed in geological surveys throughout Bushehr City are consistent with the speculative data, but significant differences can be observed considering the locations of boreholes in the area. Accordingly, the studied area is divided into several distinct parts:

- **Western region of Bushehr City**

This part consists of 2 main layers. The first layer is 1 to 2 meters thick and consists of sandy and sandy-silt soil with low density. The second layer, 10 meters thick, is a layer of sandy and silty

sediments with average density, which is located on a clayey layer. The SPT values varies from 20 to 30 in the first layer and from 30 to 50 in the second one. The water table varies from 2 to 3 meters depending on topographic situation. According to boreholes data, the cap rock layer and the third layer do not exist in this part.

- **Southern, Central and Eastern regions**

In these regions, 4 distinct layers can be observed: a) A thin layer less than 1 meter thick, b) A layer of sand 2 to 5 meters thick and with SPT values of about 20 to 30, c) Dense cemented sand layers 2 to 5 meters thick and with SPT values greater than 50, described in some geotechnical reports as coral sandstone, and d) Sandy-silt layers 3 to 5 meters thick and with SPT values in the range of 30 to 50. Furthermore, there is a layer that extends to a depth of more than 40 meters. In total, the first four layers are 9 to 14 meters thick, increasing from the north to the south. The water table varies from 2 to 3 meters depending on topographic situation. In a general view, the soil layers are summarized in Table 1.

3.2. Data and data processing

According to the results of geotechnics, downhole, refraction, geo- electric and microtremor measurement, the natural frequency from the HVSR spectral ratio curve is compared with the geotechnical parameters. To complete the study, out of the 32 geotechnical specimens, there were 27 boreholes which were near to microtremor stations.

Table 1 shows the soil profile at the point stations in Bushehr City. From the total, 32 points were recorded in the Bushehr area.

At the Bushehr site, from the obtained HVSR curve, 27 cases have clear peaks and 5 points are flat and without peaks and do not have good magnification. The presence of the peaks indicates that the amplification of the waves with a coefficient over 1.5 is clearly in the 2 Hz frequency range. Geophysical studies of downhole, refraction and electrical resistivity show that in the surface layer where the thickness is 1 to 2 meters, the shear wave velocity is about 200 m/s. The electrical resistance of this layer is between 2 and 3 Ohms. The second layer has a thickness of 2 to 6 meters, and a shear wave velocity of 480 to 1200 m/s, with the predominant value of 600 m/s. The electrical resistivity of this layer in the unsaturated regions is about 150 to 200 Ohms and in the saturation environment it is about 600 Ohms. The third layer, at depths of more than 8 m, is clay and marl, saturated with a shear velocity of about 550 m/s and an electrical resistance of about 1400 Ohms.

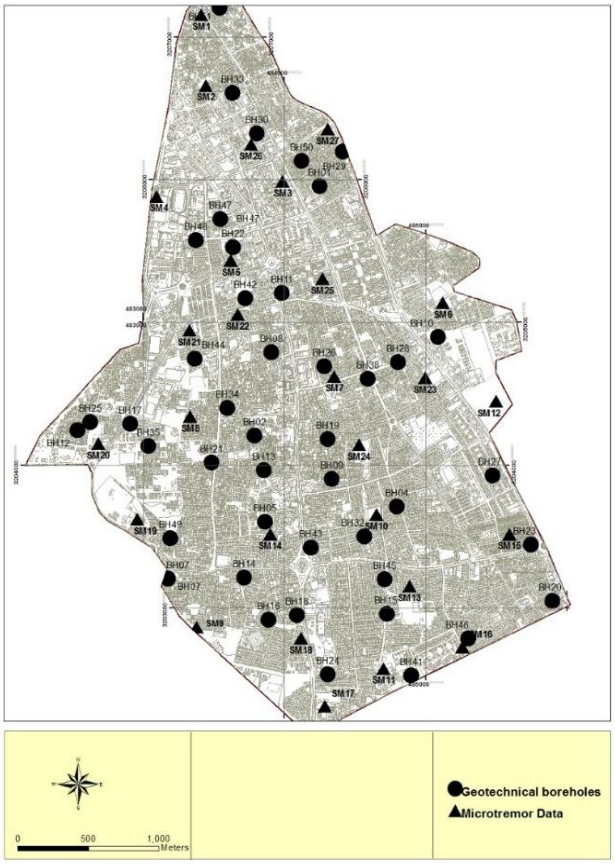

Figure 2. Location of selected stations in the studied area in Bushehr City

Microtremor measurements were taken at 27 points in the Bushehr region. For all stations the microtremors were measured and the HVSR spectral ratios were calculated by the procedure used in the Geopsy software packages prepared by the SESAME group. These measurements were performed by sampling the frequencies at 100 samples per second. Noise windows were selected automatically and were used for analysis with an overlap of 20–50 seconds between windows for 10% (cosines taper). On each window of each component Fourier spectrum analysis is then performed. Fourier spectrum analysis changes the time domain data series to a frequency domain sequence.

Table 1. Soil layers and geotechnical properties of soil layers in Bushehr area

Layer type	Layer Specification	Thickness (m)	SPT	Vs	Electrical Resistance(Ohm)
Surface soils	SP-SM	0-2	<30	200	2-3
Cap Rock	CL	2-6	>50	400-1200	150-200
Sandstone	SM	3-15	Dry: >50	500	1400
			Saturate: 20-30	500	1400
Marl-Clay	ML	>35	Dry: >50	550	1500
			Saturate: >10	550	1500

Because the data are in the form of area, the Fourier spectrum analysis uses a Fast Fourier Transform algorithm (FFT). A smoothing process is done using pieces of smoothing filters according to Konno and Ohmachi (1998), with a bandwidth of 40 coefficients that are already in the filter data, analyzed by the method of the HVSR obtained from the square root of the amplitude of the horizontal Fourier spectrum (North- South and East-West), divided by the vertical Fourier spectrum [11]. Finally, we can get the average value and standard deviation HVSR. For each station the predominant frequencies (f0) from the HVSR spectrum curve were estimated. Figures 3.a to 3.u show the selected points of HVSR curves which illustrate clear frequencies and amplitude.

From these two parameters the vulnerability index can be obtained, and mathematically written as Eq.(1) [12]:

$$Kg = \frac{A_m^{\,2}}{f_o} \qquad (1)$$

where A_m is the value of amplification and f0 is the predominant frequency.

4. Results and discussion

To evaluate the liquefaction potential in the region of Bushehr, the microtremor data and geotechnical properties of soil layers from 27 different stations from different sources were collected. The predominant frequency, site amplification coefficient and the vulnerability index were calculated. The zoning maps of each parameter were prepared and drawn individually. The vulnerability index Kg and the liquefaction safety factor (CRR) from the traditional methods were calculated. Finally, the correlation between the parameters of the HVSR and the liquefaction potential was estimated. The following describes the process of finding the correlated relation.

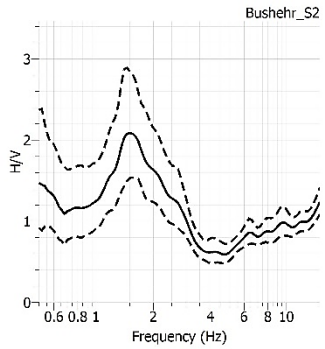

(a)

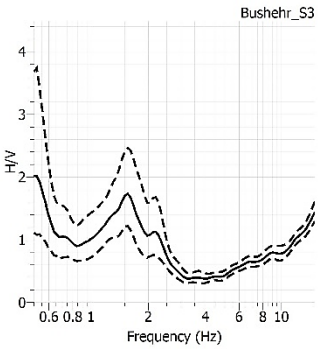

(b)

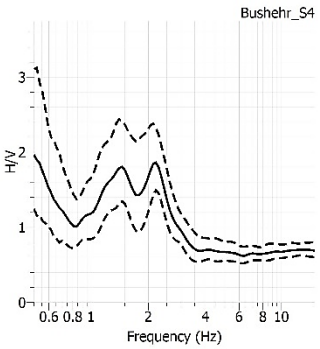

(c)

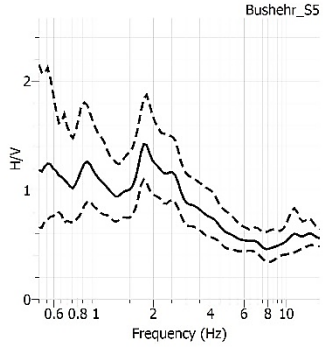

(d)

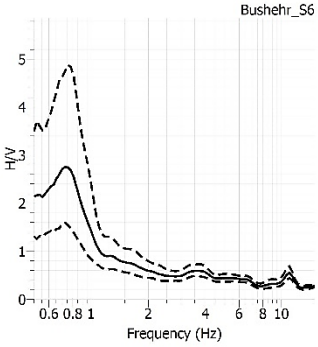

(e)

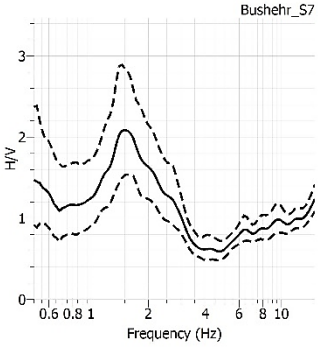

(f)

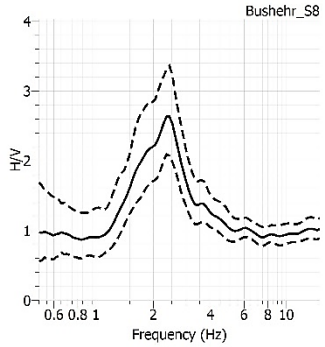

(g)

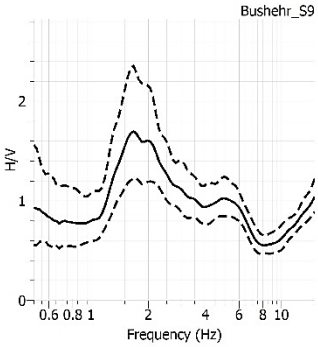

(h)

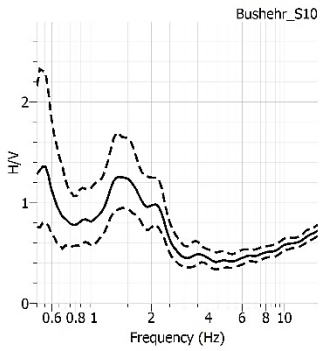

(i)

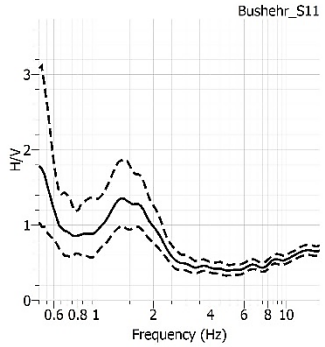

(i)

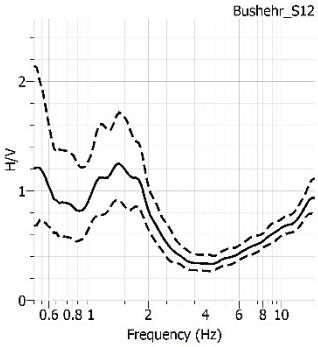

(k)

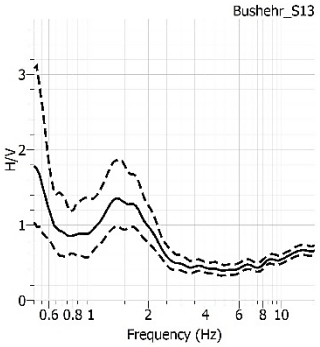

(l)

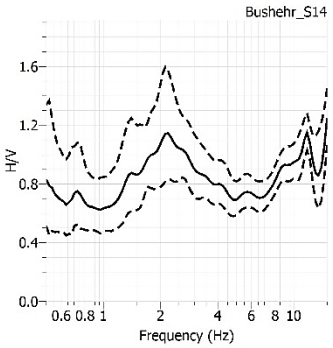

(j)

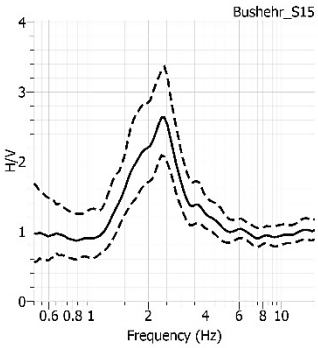

(k)

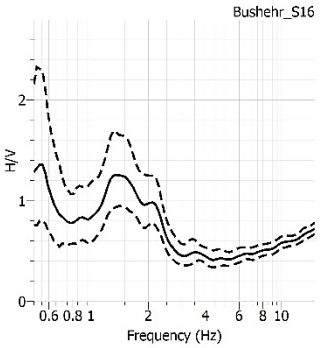

(l)

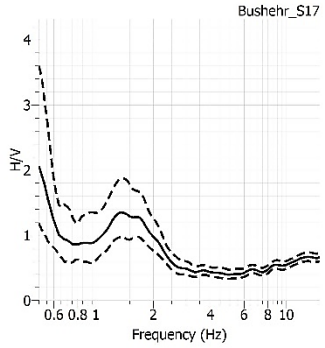

(m)

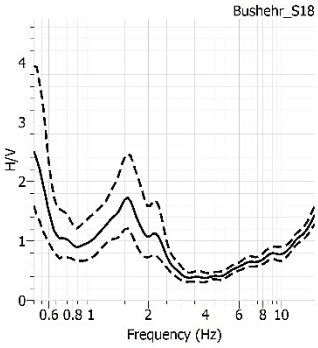

(n)

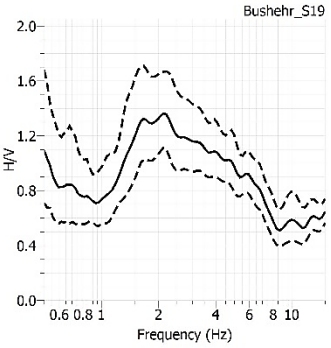

(o)

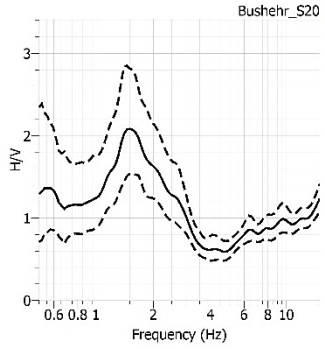

(p)

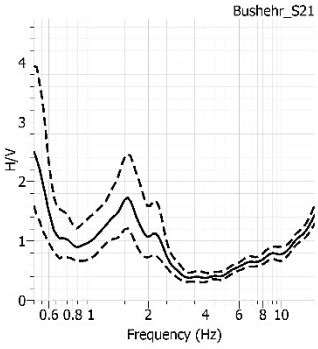

(q)

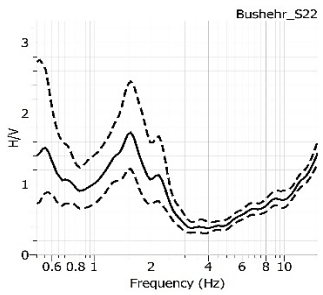

(r)

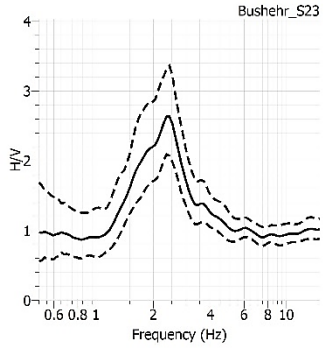

(s)

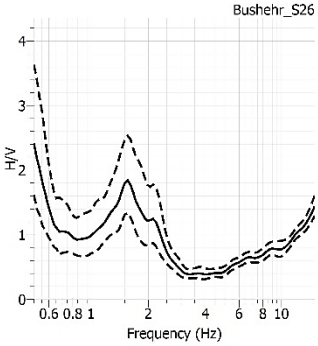

(t)

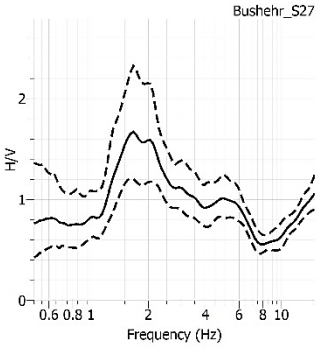

(u)

Figure 3. H/V spectral ratio curve from studied stations

4.1. Distribution of natural frequency value

The distribution maps of natural frequencies obtained from the HVSR curves in the coastal areas of Bushehr City are illustrated in Fig. 4. According to researchers, the natural frequency of the HVSR depends on the depth of the bedrock [13]; [14]; [15].

[16] and [17] showed that the natural frequency is affected by two very significant parameters, namely shear wave velocity (Vs) and bedrock depth. In addition, [13] and [18] confirmed that the natural frequency is related to the average Vs and inversely to the thickness layer (h).

According to Fig. 4, the range of natural frequency values is from 0.8 Hz to 2.4 Hz. The distribution of the natural frequency values is closely related to the geological conditions in the area. The values of the natural frequencies in the east and south of the site, or rather near the beach, are quite low, about 0.8 Hz. This means that this area has the possible form of soft ground and has a high sediment thickness. According to geologic data, this location is an alluvial area, which formed as a result of the overflow of the sea. With its low natural frequency value, this area is very prone to the occurrence of multi-reflection body waves or trapping seismic waves in the sediment. This will potentially cause great damage and also allow the occurrence of soil liquefaction [12, 19].

These parameters increase from 0.8 to 2.4 Hz from south to center of city. The values of the natural frequency in the north varies from 1.8 to 2.4 Hz. In the central part of city, which consists of the ancient downtown, the value of the natural frequency is higher than elsewhere. According to geotechnical data, the eastern region's geological conditions include siltstone, which matches the micro tremor data. The natural frequencies in this area are quite low and it has a low level of multi-reflection body wave sediment layers.

4.2. Distribution of amplification factor

The results of the amplification value distribution map in Fig. 5 show that the values of amplification in the overlying Bushehr coastal region range from 1.1 to 2.7, which are in the moderate to high amplification range[20]. This value indicates the strengthening of waves that propagate in the sediment. The amplification is influenced by the value of shear wave velocity Vs, with significant contrast of the sediment and bedrock descriptions [18]. The amplification values in the central part are from 1.5 to 2.4. Nakamura et al. (2000) showed that the amplification parameters that can damage buildings have values greater than 3. This is also supported by Huang and Tseng (2002). Thus, it cannot be said that areas with moderate amplification values, which are far from the coast, are potential danger areas, and another parameter is required to be able to connect the natural frequency and amplification in characterizing the soil layers. Distribution of vulnerability index

The vulnerability index or so-called Kg value has been described in Eq. (1). This equation is used to identify areas susceptible to strong ground motion that, [21]; [11]; Konno and Ohmachi, 1998; Huang and Tseng, 2002). This vulnerability index can link the natural frequency and amplification values.

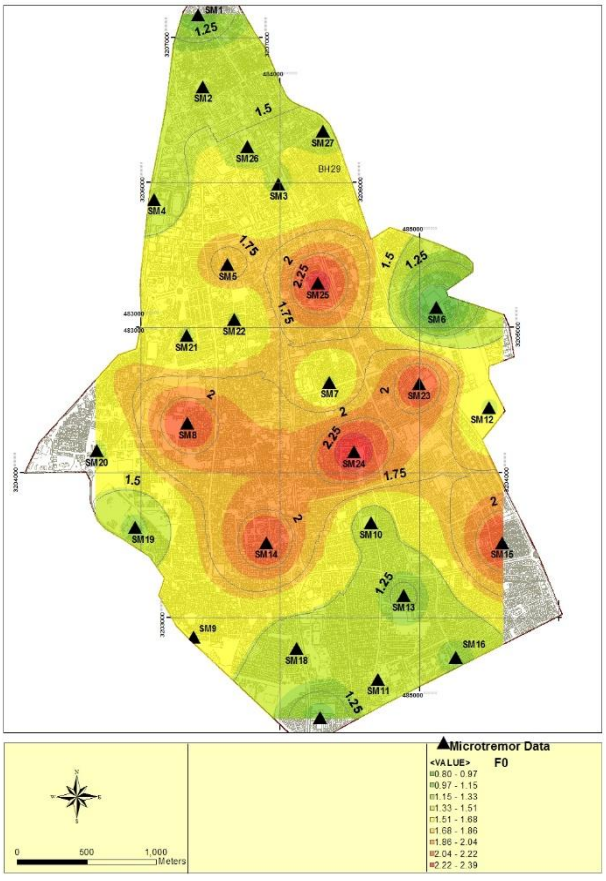

Figure 4. Distribution map of predominant frequency

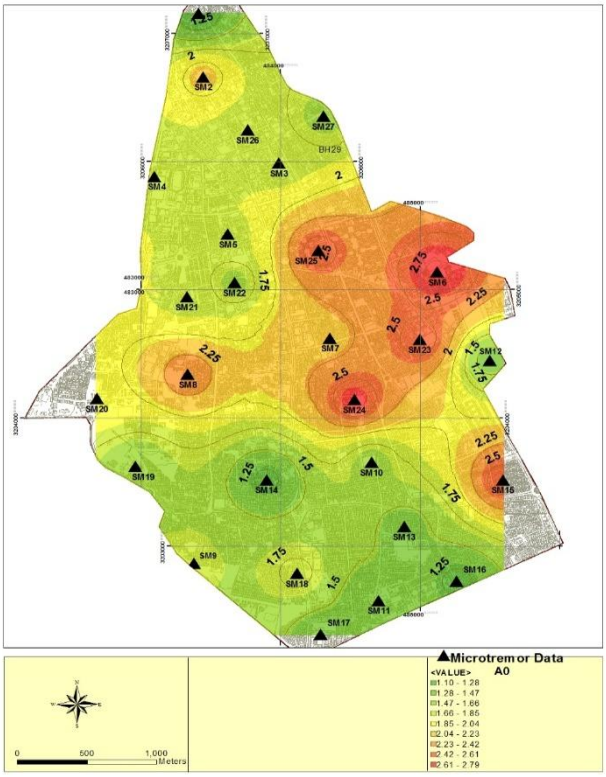

Figure 5. Distribution map of amplification factor

Huang and Tseng (2002) used this to map the alluvial fan area of Yuan Lin in Taiwan and showed that generally high vulnerability values can potentially have soil liquefaction. Using the Kg value, Mokhberi (2015), suggested an approach to evaluate the building damage rate and disaster measurement [22]. From the results of calculations using the equations introduced by Nakamura (2000), the Kg values obtained in the coastal region of Bushehr are from 0.7 to 9.8. In Fig. 6, along the eastern part of Bushehr region the value of the vulnerability index is quite high at 1.5 to 9. If correlated with the value of the natural frequency and the high amplification value, the eastern part is the area with the most potential for liquefaction to occur. In the north (point's SM11, SM13, SM14, and SM16) the values range from 0.7 to 1.7. Compared to the other parts, this value is quite small. It can be concluded that the northern region has a low potential for soil liquefaction.

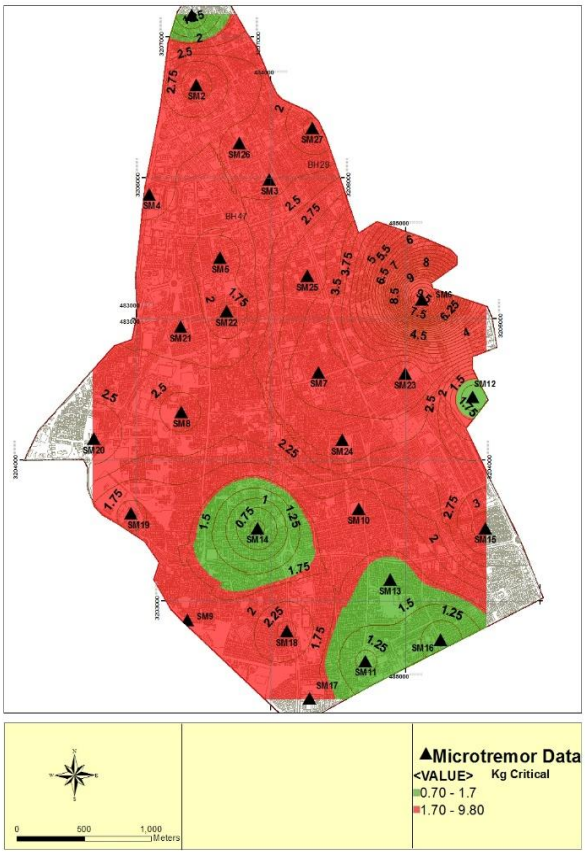

Figure 6. Distribution map of vulnerability index in Bushehr area

4.3. Liquefaction potential assessment using standard penetration test (SPT) method.

The liquefaction potential estimation based on the Vs [23] and SPT [24] has required the level of dynamic loading excited by the earthquake, (CSR), overburden pressure, shear wave velocity, Vs, and the resistance of the soil to liquefaction, (CRR). Following describes the different procedure of mentioned parameter [25].

4.3.1. Cyclic Stress Ratio (CSR)

The cyclic stress ratio at a depth i can be determined by Eq.(2) [4].

$$\mathrm{CSR}_{7.5} = 0.65\left(\frac{a_{max}}{g}\right)\left(\frac{\sigma_{v0}}{\sigma'_{v0}}\right)\mathrm{rd} \qquad (2)$$

$$r_d = \left(\frac{1.000-0.4113z^{0.5}+0.04052z+0.001753z^{1.5}}{1.000-0.4177z^{0.5}+0.05729z-0.005205z^{1.5}+0.001210z^{2}}\right) \qquad (3)$$

where, amax is maximum acceleration, g is the acceleration of gravity, σ_{v0} and σ'_{v0} are total and effective stress respectively, z is the depth and rd is the shear stress reduction coefficient.

4.3.2.Cyclic Resistance Ratio (CRR)

The cyclic resistance ratio (CRR) has been measured by the procedure recommended by Seed and Idris (1971). In this method, the value of CRR obtain from three related factors described in Eqe.3 (4) to (8) [26]. the burden pressure factor R1, soil moisture content factor R2 and fine part of soil.

$$CRR=R_1+R_2+R_3 \quad (4)$$

$$R1 = 0.0882\sqrt{\frac{N_j}{\sigma'_v+0.7}} \quad (5)$$

$$R2 = \begin{cases} 0.19 & 0.02mm < D_{50} < 0.05mm \\ 0.22\ log\frac{0.35}{D_{50}} & 0.05mm < D_{50} < 0.6mm \\ -0.05\ 0.02mm < D_{50} < 0.05mm & \end{cases} \quad (6)$$

$$R3 = \begin{cases} 0.0 & 0\% < FC < 40\% \\ 0.004FC - 0.16 & 40\% < FC < 100\% \end{cases} \quad (7)$$

$$N_j = 0.833(N_1)_{60} \quad (8)$$

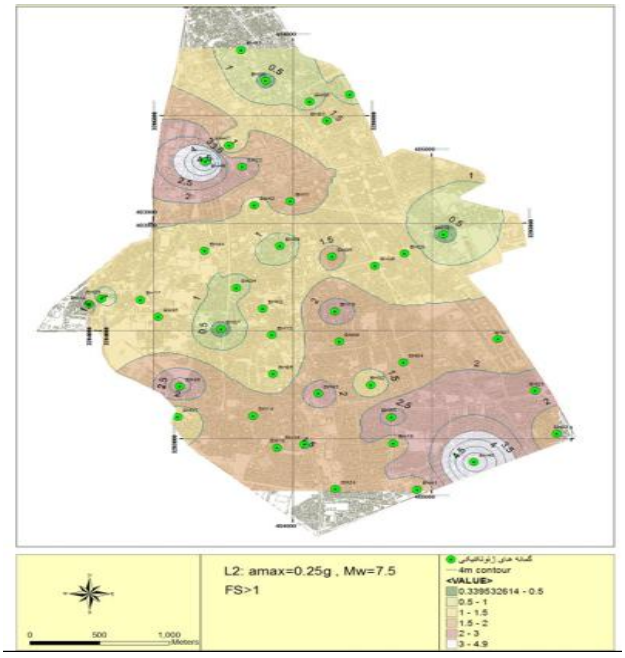

Figure 7. Liquefaction potential distribution map for hazard risk level L1

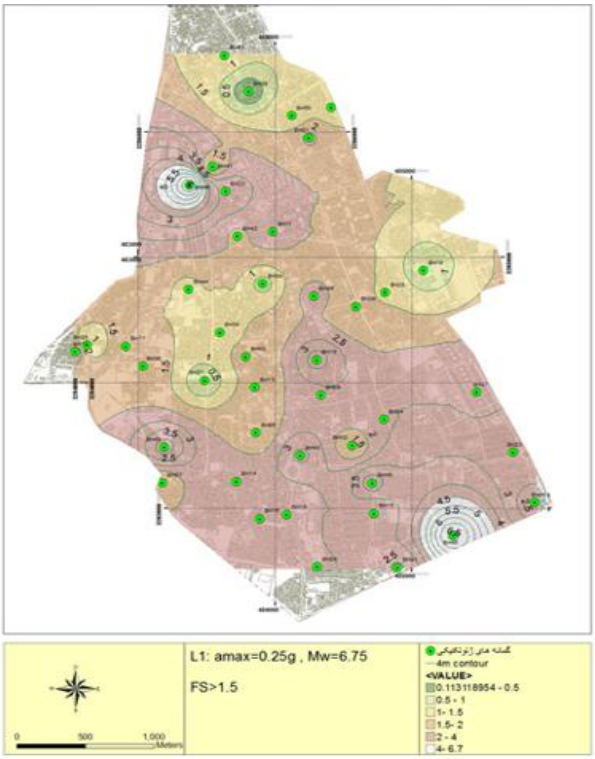

Figure 3 Liquefaction potential distribution map for hazard risk level L2

Where Nj is the SPT Number in the Geotechnical Japan Standards, D50 is the average diameters of aggregate and FC is Fine grain percent. In order to quantify the liquefaction potential, the safety factor has been used. The factor of safety (FS) against liquefaction is measured using the Eq. (8) [27], where CRRJ is the corrected value of CRR estimated through Eq. (4). Using this criterion, it is clear that the liquefaction occurs if FS ≤1 and does not occur when FS > 1:

$$\boldsymbol{FS = \frac{CRR_j}{CSR}} \quad (9)$$

Table 2. Bore hole, microtremor and vulnerability indexes data that used in liquefaction evaluation

Bushehr City										
Station	BH No	f	A	Kg	NSPT	CSR	CRR 7.5	CRR 6.5	FS1	FS2
S1	BH51	1.1	1.1	1.1	26	0.294	0.13	0.176	0.44	0.60
S2	BH33	1.5	2.1	2.9	24	0.267	0.62	0.845	2.32	3.16
S3	BH01	1.5	1.8	2.2	36	0.26	0.46	0.623	1.77	2.40
S4	BH47	1.4	1.8	2.3	29	0.3	1.05	1.431	3.50	4.77
S5	BH22	1.8	1.8	1.8	28	0.3	0.45	0.613	1.50	2.04
S6	BH10	0.8	2.8	9.8	36	0.26	0.46	0.627	1.77	2.41
S7	BH26	1.5	2.2	3.2	33	0.3	0.59	0.801	1.97	2.67
S8	BH21	2.2	2.4	2.6	14	0.3	0.55	0.748	1.83	2.49
S9	BH07	1.6	1.7	1.8	16	0.26	0.46	0.627	1.77	2.41
S10	BH32	1.4	1.6	1.8	29	0.31	0.52	0.708	1.68	2.28
S11	BH41	1.4	1.3	1.2	44	0.34	0.32	0.431	0.94	1.27
S12	BH27	1.5	1.4	1.3	27	0.3	0.66	0.899	2.20	3.00
S13	BH15	1.2	1.4	1.6	44	0.3	0.38	0.518	1.27	1.73
S14	BH05	2.2	1.2	0.7	26	0.293	0.13	0.18	0.44	0.61
S15	BH23	2.2	2.6	3.1	36	0.26	0.72	0.98	2.77	3.77
S16	BH46	1.3	1.2	1.1	24	0.293	0.13	0.18	0.44	0.61
S17	BH24	1.1	1.4	1.8	44	0.34	1.2	1.63	3.53	4.79
S18	BH18	1.4	1.8	2.3	24	0.264	0.62	0.84	2.35	3.18
S19	BH49	1.3	1.5	1.7	24	0.26	0.6	0.82	2.31	3.15
S20	BH12	1.5	2	2.7	36	0.26	0.46	0.63	1.77	2.42
S21	BH44	1.5	1.8	2.2	36	0.26	0.72	0.98	2.77	3.77
S22	BH42	1.5	1.6	1.7	44	0.31	0.168	0.19	0.54	0.61
S23	BH28	2.2	2.6	3.1	15	0.264	0.292	0.43	1.11	1.63
S24	BH19	2.4	2.5	2.6	44	0.31	0.339	0.46	1.09	1.48
S25	BH11	2.3	2.6	2.9	44	0.33	0.38	0.52	1.15	1.58
S26	BH30	1.5	1.8	2.2	40	0.3	0.45	0.61	1.50	2.03
S27	BH29	1.5	1.6	1.7	33	0.296	0.14	0.18	0.47	0.62

4.4. Reliability assessment of liquefaction potential obtained from vulnerability index

Based on the TC4 classification approach, two levels of L1 (amax = 0.25,

M = 6.75, FSmin = 1.5) and L2 (amax = 0.25, M = 7.5, FSmin = 1) are considered. Using the relationships (2) and (3), proposed by the National Center for Earthquake Engineering Research, NCEER, the reliability coefficient for the two levels of L1 and L2 have been calculated for all boreholes and, at different depths[28].

The geotechnical specification of soil layers at selected stations have been summarized in Table 2. According to the geotechnical investigation, the first two layers are a sandy soil (SP-ML) 2 to 8 meters thick. Using the ArcGIS software, the safety factor contour line for the two risk levels L1 and L2 at the hazardous depths

are calculated. The contour lines have been plotted on the Bushehr map. Figures 7 and 8 show the maps of the liquefaction potential based on the SPT data and are visible for the two L1 and L2 risk levels.

The contour lines of the liquefaction factor of safety for risk level L1 and l2 have been illustrated in Fig. 7 and Fig. 8 respectively. The safety factor varies from 0.44 to 3.5 in risk level 1 and from 0.6 to 4.8 in risk level 2 for the deeper liquefiable depth. Given the fact that in the risk level a safety factor of less than 1.5 indicates that the areas are susceptible to liquefaction, for the depths of 4 to 6 meters, the central and Sothern parts of the city are prone to liquefaction. Therefore, in all districts of Bushehr City, except for a part on the north side, the soil layers are more prone to liquefaction hazard, and the hazard level 2, L2, is more susceptible than L1.

4.5. Comparison of liquefaction potential evaluation of geotechnical and microtremor methods

From reviewing the past scientific literature, it is concluded that the larger the value of Kg, the greater the liquefaction potential. In fact, the proposed value of Kg has a qualitative aspect, and it is certainly not possible to ensure that the boundary of Kg determines the liquefaction potential. It can be said that each region has a special Kg. Investigation of the liquefaction potential using geotechnical data and comparing the results with Kg values obtained from microtremors, were performed. The Kg values obtained from the 27 microtremor stations are compared with the results of liquefaction of the 27 geotechnical boreholes. Table 2 shows that at all the microtremor stations with Kg equal to or greater than 1.7 liquefaction occurred. Therefore, we can consider the value of Kg equal to 1.7 as the basis for estimating the liquefaction potential of Bushehr City. In other words, for all stations with Kg greater than 1.7 there is a probability of liquefaction, and for stations with Kg less than 1.7, the potential occurrence of liquefaction potential is low. Given the critical Kg value, the 1.7 value is mapped to the vulnerability index map in ArcGIS software, and a zoning map is fitted to this value. For wide areas of Bushehr City, with the exception of segments of the regions of the northern part, the Kg values are higher than 1.7.

5. Conclusion

Microtremor data is a tool which is used in site effect determination. In this study to obtain information on the characteristics of subsoils in Bushehr City, microtremor measurements were performed. Using the HVSR technique, the predominant frequency and amplification factor at each point were determined. The Kg value, a derivative of the two mentioned parameters and supposedly an index of the vulnerability of the ground to earthquake hazards, was also estimated. Of the corresponding distribution maps that have been generated, the frequency distribution map correlates well with the geology of the study area. This investigation is compared with the geotechnical data. From the analysis and interpretation of the above data, the following deductions can be made:

1. The results show that the HVSR technique reliably identifies the sites' predominant frequency and amplification factors. The site classification map was then combined with the preliminary liquefaction vulnerability map derived from the traditional approach, using the geotechnical approach to generate an integrated liquefaction hazard map of Bushehr City.
2. This map is believed to be more accurate in illustrating the relative liquefaction susceptibility since it combines information on the distribution of potentially liquefiable soils in terms of soil layer specifications and information on the thickness and stiffness of these soils.
3. Using the information about the thickness of the sedimentary cover, an idea of the severity of liquefaction-related damage can also be gathered since thicker deposits relate to more serious damage. Moreover, together with the soil specification, the layer thickness controls the amplification, and these are among the most important factors controlling the occurrence of liquefaction.
4. With the use of the vulnerability index, Kg, derived from the microtremor HVSR curve, the accuracy of the liquefaction liability evaluation and zonation is much improved. It should be noted that the accuracy of the soil layers liquefaction susceptibility map is

improved by supplementing it with subsurface data obtained from SPT.

5. Alongside the geotechnical methods, this microtremor- based approach is useful in site characterization studies due to its easy use and low budget. Thus, generally, extrapolations are simply made from limited and scattered subsurface data and similar subsurface conditions are just assumed for the same geologic/geomorphic units.
6. The vulnerability index for Bushehr City ranged from 0.7 to 9.8. The value of 1.7 can be selected as the critical vulnerability index which separates the liquefiable and non-liquefiable areas. Four areas have a high potential for soil liquefaction, with a small natural frequency, high amplification and high vulnerability index. These areas are continued from east to west, as well as the southern region.
7. An area with a low potential for soil liquefaction is located in western Bushehr, having a high natural frequency, low amplification and low vulnerability index.

6. References

[1] Nakamura, Y., A method for dynamic characteristics estimation of subsurface using microtremor on the ground surface, in Quarterly Report Railway Tech. Res. Inst. 1989. p. 25-30.

[2] Tuladhar, R., et al., Seismic microzonation of the greater Bangkok area using microtremor observations. Earthquake engineering & structural dynamics, 2004. 33(2): p. 211-225.

[3] Walter, T., et al., The 26 May 2006 magnitude 6.4 Yogyakarta earthquake south of Mt. Merapi volcano: Did lahar deposits amplify ground shaking and thus lead to the disaster? Geochemistry, Geophysics, Geosystems, 2008. 9(5).

[4] Seed, H.B. and I.M. Idriss, Simplified procedure for evaluating soil liquefaction potential. Journal of Soil Mechanics & Foundations Div, 1971.

[5] Lermo, J. and F.J. Chávez-García, Site effect evaluation using spectral ratios with only one station. Bulletin of the Seismological Society of America, 1993. 83(5): p. 1574-1594.

[6] Teves-Costa, P., L. Matias, and P. Bard, Seismic behaviour estimation of thin alluvium layers using microtremor recordings. Soil Dynamics and Earthquake Engineering, 1996. 15(3): p. 201-209.

[7] Seed, H.B. and P. De Alba. Use of SPT and CPT tests for evaluating the liquefaction resistance of sands. in Use of in situ tests in geotechnical engineering. 1986. ASCE.

[8] Robertson, P., D. Woeller, and W. Finn, Seismic cone penetration test for evaluating liquefaction potential under cyclic loading. Canadian Geotechnical Journal, 1992. 29(4): p. 686-695.

[9] Harder Jr, L.F., Application of the Becker penetration test for evaluating the liquefaction potential of gravelly soils. 1997.

[10] www.en.wikipedia.org. Bushehr_earthquake. 2013.

[11] Nakamura, Y. Clear identification of fundamental idea of Nakamura's technique and its applications. in Proceedings of the 12th world conference on earthquake engineering. 2000. Auckland New Zealand.

[12] Nakamura, Y. Clear identification of fundamental idea of Nakamura's technique and its applications. in Proceedings of the 12th world conference on earthquake engineering. 2000. Auckland New Zealand.

[13] Parolai, S., P. Bormann, and C. Milkereit, New relationships between Vs, thickness of sediments, and resonance frequency calculated by the H/V ratio of seismic noise for the Cologne area (Germany). Bulletin of the seismological society of America, 2002. 92(6): p. 2521-2527.

[14] Chen, Q., et al., Site effects on earthquake ground motion based on microtremor measurements for metropolitan Beijing. Chinese Science Bulletin, 2009. 54(2): p. 280-287.

[15] Mokhberi, M., et al., Experimental evaluation of the H/V spectral ratio capabilities in estimating the subsurface layer characteristics. Iranian Journal of Science and Technology.

Transactions of Civil Engineering, 2013. 37(C): p. 457.

[16] Sato, T., Y. Nakamura, and J. Saita. The change of the dynamic characteristics using microtremor. in The 14 th World Conference on Earthquake Engineering. 2008.

[17] Gosar, A., et al., Microtremor study of site effects and soil-structure resonance in the city of Ljubljana (central Slovenia). Bulletin of earthquake engineering, 2010. 8(3): p. 571-592.

[18] Sungkono, D.D.W. and W.U. Triwulan, Evaluation of buildings strength from microtremor analyses. structure, 2011. 6: p. 8.

[19] Huang, H.-C. and Y.-S. Tseng, Characteristics of soil liquefaction using H/V of microtremors in Yuan-Lin area, Taiwan. Terrestrial, Atmospheric and Oceanic Sciences, 2002. 13(3): p. 325-338.

[20] Horike, M., B. Zhao, and H. Kawase, Comparison of site response characteristics inferred from microtremors and earthquake shear waves. Bulletin of the Seismological Society of America, 2001. 91(6): p. 1526-1536.

[21] Nakamura, Y. Seismic vulnerability indices for ground and structures using microtremor. in World Congress on Railway Research in Florence, Italy. 1997.

[22] Mokhberi, M., Vulnerability evaluation of the urban area using the H/V spectral ratio of microtremors. International journal of disaster risk reduction, 2015. 13: p. 369-374.

[23] Andrus, R.D., et al., Comparing liquefaction evaluation methods using penetration-VS relationships. Soil dynamics and earthquake engineering, 2004. 24(9-10): p. 713-721.

[24] Bolton Seed, H., et al., Influence of SPT procedures in soil liquefaction resistance evaluations. Journal of Geotechnical Engineering, 1985. 111(12): p. 1425-1445.

[25] Khalili Noutash, M., R. Dabiri, and M. Hajialilue Bonab, Evaluating the Liquefaction Potential of Soil in the South and Southeast of Tehran based on the Shear Wave Velocity through Empirical Relationships. Journal of Structural Engineering and Geo-Techniques, 2012. 2(1): p. 29-41.

[26] Iwasaki, T. A practical method for assessing soil liquefaction potential based on case studies at various sites in Japan. in Proc. Second Int. Conf. Microzonation Safer Construction Research Application, 1978. 1978.

[27] Baxter, C.D., et al., Correlation between cyclic resistance and shear-wave velocity for providence silts. Journal of geotechnical and geoenvironmental engineering, 2008. 134(1): p. 37-46.

[28] Cetin, K.O., et al., Standard penetration test-based probabilistic and deterministic assessment of seismic soil liquefaction potential. Journal of geotechnical and geoenvironmental engineering, 2004. 130(12): p. 1314-1340.